*Inorg. Chem.* **1993,** *32,* 811–815

# Pyridine-2-thiolate Binding of Osmium(III). Geometrical Isomers of $[Os(C_5H_4NS)_2(PPh_3)_2]PF_6 \cdot nH_2O$ ($n$ = 1, 0)[†]

**Amitava Pramanik, Nilkamal Bag, and Animesh Chakravorty***

Department of Inorganic Chemistry, Indian Association for the Cultivation of Science,
Calcutta 700 032, India

*Received May 27, 1992*

Oxidation of $OsL_2(PPh_3)_2$ by cerium(IV) has afforded the first osmium(III) complex of pyridine-2-thiol (HL), $[OsL_2(PPh_3)_2]PF_6 \cdot nH_2O$, in two geometrically isomeric forms of green ($n$ = 1) and red ($n$ = 0) color, the latter being a minor (~1%) constituent. It is proposed that the oxidation process preserves the original isomer population present in solutions of the osmium(II) precursor in the form of stereorigid osmium(III). Structure determination has revealed that the $OsN_2S_2P_2$ coordination sphere has cis-cis-trans (*cct*) and trans-trans-trans (*ttt*) geometries in the green and the red forms respectively: *cct* space group $P2_1/c$, $Z = 4$, $a = 10.265(2)$ Å, $b = 22.289(8)$ Å, $c = 19.881(10)$ Å, $\beta = 102.85(3)°$, $V = 4435(3)$ Å$^3$; *ttt* space group $C2/c$, $Z = 8$, $a = 23.615(10)$ Å, $b = 20.605(6)$ Å, $c = 19.440(5)$ Å, $\beta = 94.19(3)°$, $V = 9434(5)$ Å$^3$. The *ttt* complex is centrosymmetric, and the $OsL_2$ fragment is excellently planar with an average Os–S distance of 2.374(3) Å. In the *cct* isomer the two planar OsL moieties make a dihedral angle of 12.7° and the average Os–S distance is 2.395(3) Å. It is proposed that there is significant cis-thiolato repulsion in the *cct* isomer. Both isomers afford rhombic EPR spectra which have been analyzed using the **g**-tensor theory of low-spin $d^5$ ions. The predicted ligand-field transitions within the $t_2$ shell are observed: *cct*, 7400 cm$^{-1}$; *ttt*, 8300 cm$^{-1}$. The osmium(III)–osmium(II) reduction potentials are 0.14 V (*cct*), and –0.11 V vs SCE (*ttt*). Stronger back-bonding within the $OsL_2$ fragment in *cct*-$OsL_2(PPh_3)_2$ than that in the *ttt* isomer may be one of the factors responsible for this inequality. Of the three possible isomers (*ctc*, *tcc*, *ccc*) with the sterically unfavorable *cis*-$(PPh_3)_2$ configuration none are observed for the osmium(III) complex; the osmium(II) precursor however has the *ctc* configuration in the solid state.

## Introduction

This work stems from our interest in geometrically isomeric osmium(II,III) complexes of type $Os(bidentate)_2(PPh_3)_2$. Thus far our studies were limited to symmetrical bidentate ligands of the SS donor type.[1–3] In this work we examine the first osmium(III) case where the bidentate ligand is unsymmetrical leading to a larger number of possible isomers. The concerned ligand is pyridine-2-thiol (HL) whose platinum metal chemistry is receiving significant current attention.[4–8] In the particular case of osmium, a number of HL complexes of the bivalent metal are documented,[9–12] but nothing is known about the higher valent species.

Herein we describe the preparation and properties of the first osmium(III) complex of HL which also belongs to the required bis-bidentate bis(phosphine) type: $[OsL_2(PPh_3)_2]PF_6 \cdot nH_2O$ ($n$ = 0, 1). It occurs in two isomeric forms which have been separated and structurally characterized. Electronic distortions of the metal environments are probed with the help of EPR and near-IR spectra. Isomeric interrelationships with an osmium(II) precursor are examined.

## Results and Discussion

**A. Synthesis.** The bivalent precursor complex $OsL_2(PPh_3)_2$[10] was prepared in ~100% yield by a new route utilizing $OsBr_2(PPh_3)_3$ and HL. Upon reaction of a solution of $OsL_2(PPh_3)_2$ in dichloromethane–acetonitrile mixture with a slight excess of aqueous cerium(IV), very rapid oxidation occurs forming $OsL_2(PPh_3)_2^+$ (eq 1). It is isolated in nearly quantitative yield as the $PF_6^-$ salt. Careful recrystallization of the green colored salt afforded discrete green ($n$ = 1) and red ($n$ = 0) crystals of composition $[OsL_2(PPh_3)_2]PF_6 \cdot nH_2O$. These were separated by hand-picking. The red complex constituted only ~1% of the total mass. Selected characterization data for the two complexes

$$OsL_2(PPh_3)_2 + Ce(IV) \rightarrow OsL_2(PPh_3)_2^+ + Ce(III) \qquad (1)$$

---

[†] Dedicated to Professor Richard H. Holm on the occasion of his 60th birthday.

(1) Pramanik, A.; Bag, N.; Ray, D.; Lahiri, G. K.; Chakravorty, A. *Inorg. Chem.* **1991**, *30*, 410–417.

(2) Pramanik, A.; Bag, N.; Ray, D.; Lahiri, G. K.; Chakravorty, A. *J. Chem. Soc., Chem. Commun.* **1991**, 139–141.

(3) Pramanik, A.; Bag, N.; Lahiri, G. K.; Chakravorty, A. *J. Chem. Soc., Dalton Trans.* **1992**, 101–105.

(4) (a) Yamamoto, J. H.; Yoshida, W.; Jensen, C. M. *Inorg. Chem.* **1991**, *30*, 1353–1357. (b) Umakoshi, K.; Ichimura, A.; Kinoshita, I.; Ooi, S. *Inorg. Chem.* **1990**, *29*, 4005–4010. (c) Padilla, E. M.; Yamamoto, J. H.; Jensen, C. M. *Inorg. Chim. Acta* **1990**, *174*, 209–215. (d) Deeming, A. J.; Meah, M. N.; Bates, P. A.; Hursthouse, B. *J. Chem. Soc., Dalton Trans.* **1988**, 2193–2199.

(5) (a) Umakoshi, K.; Kinoshita, I.; Fukui-Yasuba, Y.; Matsumoto, K.; Ooi, S.; Nakai, H.; Shiro, M. *J. Chem. Soc., Dalton Trans.* **1989**, 815–819. (b) Umakoshi, K.; Kinoshita, I.; Ichimura, A.; Ooi, S. *Inorg. Chem.* **1987**, *26*, 3551–3556.

(6) (a) Ciriano, M. A.; Perez-Torrente, J. J.; Viguri, F.; Lahoz, F. J.; Oro, L. A.; Tiripicchio, A.; Tiripicchio-Camellini, M. *J. Chem. Soc., Dalton Trans.* **1990**, 1493–1502. (b) Deeming, A. J.; Meah, M. N.; Bates, P. A.; Hursthouse, M. B. *J. Chem. Soc., Dalton Trans.* **1988**, 235–238. (c) Deeming, A. J.; Hardcastle, K. I.; Meah, M. N.; Bates, P. A.; Dawes, H. M.; Hursthouse, M. B. *J. Chem. Soc., Dalton Trans.* **1988**, 227–233. (d) Deeming, A. J.; Meah, M. N.; Dawes, H. M.; Hursthouse, M. B. *J. Organomet. Chem.* **1986**, *299*, C25–C28.

(7) (a) Constable, E. C.; Raithby, P. R. *Inorg. Chim. Acta* **1991**, *183*, 21–23. (b) Andreu, P. L.; Cabeza, J. A.; Farnandez-Colinas, J. M.; Riera, V. *J. Chem. Soc., Dalton Trans.* **1990**, 2927–2930. (c) Baghlaf, A. O.; Ishaq, M.; Rashed, A. K. A. *Polyhedron* **1987**, *6*, 837–839. (d) Toma, H. E.; Santos, P. S.; Mattioli, M. P. D.; Oliveira, L. A. A. *Polyhedron* **1987**, *6*, 603–611. (e) Mura, P.; Olby, B. G.; Robinson, S. D. *Inorg. Chim. Acta* **1985**, *98*, L21–L22. (f) Rosete, R. O.; Cole-Hamilton, D. J.; Wilkinson, G. *J. Chem. Soc., Dalton Trans.* **1979**, 1618–1623. (g) Gilbert, J. D.; Rose, D.; Wilkinson, G. *J. Chem. Soc. A* **1970**, 2765–2769.

(8) Fletcher, S. R.; Skapski, A. C. *J. Chem. Soc., Dalton Trans.* **1972**, 635–639.

(9) Burgess, K.; Johnson, B. F. G.; Lewis, J. *J. Organomet. Chem.* **1982**, *233*, C55–C58.

(10) Mura, P.; Olby, B. G.; Robinson, S. D. *J. Chem. Soc., Dalton Trans.* **1985**, 2101–2112.

(11) Alteparmakian, V.; Mura, P.; Olby, B. G.; Robinson, S. D. *Inorg. Chim. Acta* **1985**, *104*, L5–L6.

(12) Deeming, A. J.; Meah, M. N.; Randle, N. P.; Hardcastle, K. I. *J. Chem. Soc., Dalton Trans.* **1989**, 2211–2216.

0020-1669/93/1332-0811$04.00/0

**Table I.** Electronic Spectral Data[a] and Cyclic Voltammetric Reduction Potentials[b] for Isomers at 298 K

| compd | vis–near-IR data: $\lambda_{max}$, nm ($\epsilon$, $M^{-1}\ cm^{-1}$) | Os(III)–Os(II) $E_{1/2}$, $V$ ($\Delta E_p$, mV)[c] |
|---|---|---|
| *cct*-[$OsL_2(PPh_3)_2$]$PF_6\cdot H_2O$ | 1350 (190), 690 (1700), 590 (1680), 480 (655) | 0.14 (100) |
| *ttt*-[$OsL_2(PPh_3)_2$]$PF_6$ | 1200 (85), 760 (5180), 575[d] (490), 450 (900) | –0.11 (90) |

[a] The solvent is dichloromethane. [b] Conditions: solvent, dichloromethane; supporting electrolyte, TEAP (0.1 M); working electrode, platinum; reference electrode, SCE; solute concentration, ~$10^{-3}$ M. [c] $E_{1/2} = 0.5(E_{pa} + E_{pc})$ at scan rate 50 mV $s^{-1}$, where $E_{pa}$ and $E_{pc}$ are anodic and cathodic peak potentials, respectively; $\Delta E_p = E_{pa} - E_{pc}$. [d] Shoulder.

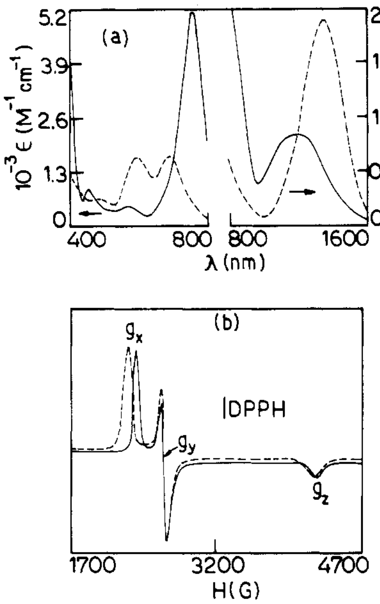

Figure 1. (a) Electronic spectra of *cct*-[$OsL_2(PPh_3)_2$]$PF_6\cdot H_2O$ (- - -) and *ttt*-[$OsL_2(PPh_3)_2$]$PF_6$ (—) in dichloromethane. (b) X-Band EPR spectra of *cct*-[$OsL_2(PPh_3)_2$]$PF_6\cdot H_2O$ (- - -) and *ttt*-[$OsL_2(PPh_3)_2$]$PF_6$ (—) in 1:1 dichloromethane–toluene glass (77 K).

are collected in Table I. The species display distinctive electronic spectra in the region 400–1600 nm (Figure 1a).

**B. Crystal and Molecular Structure.** In the green complex, the cations are of a single type with all atoms occupying general positions. In the red complex, two crystallographically distinct but metrically near-identical centrosymmetric cations are present (metal atoms at $^1/_4$, $^1/_4$, 0 and $^1/_4$, $^1/_4$, $^1/_2$). Molecular views are shown in Figures 2 and 3. Selected bond parameters are lised in Table II. In the lattice of the green isomer the water oxygen atoms are grouped in pairs (O···O = 2.846(8) Å), evidently due to hydrogen bonding. A view of the lattice down the b axis revealing the water dimers is deposited as supplementary material.

In both complexes $L^-$ is bonded in the four-membered N,S chelate mode and the metal coordination sphere is of type $OsN_2S_2P_2$. The angular distortions from ideal octahedral geometry are large (Table II). The donor pair triad (N,N)-(S,S)-(P,P) is cis-cis-trans (**1**, *cct*) in the green complex and trans-trans-trans (**2**, *ttt*) in the red complex.

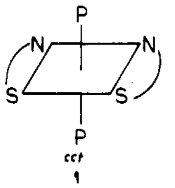

*cct*
**1**

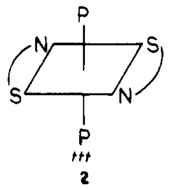

*ttt*
**2**

The $OsL_2$ fragment is excellently planar (mean deviation 0.015 Å) in both the crystallographically distinct molecules of the *ttt* isomer. This is not so in the *cct* isomer (mean deviation 0.122 Å)—the two OsL moieties are, however, separately planar (mean deviation 0.034 Å) and the dihedral angle between the two planes

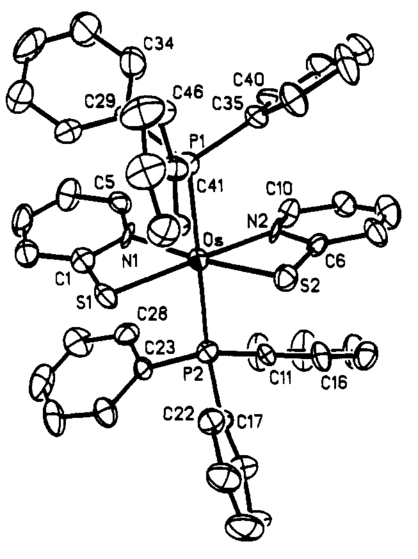

Figure 2. ORTEP plot (40% probability ellipsoid) and labeling scheme for the cation of *cct*-[$OsL_2(PPh_3)_2$]$PF_6\cdot H_2O$.

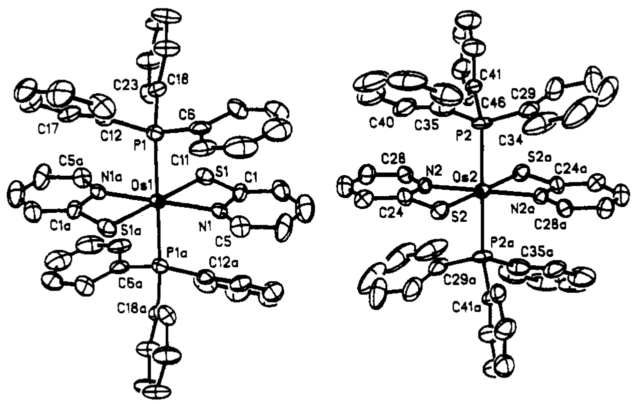

Figure 3. ORTEP plot (40% probability ellipsoid) and labeling scheme for the cation of *ttt*-[$OsL_2(PPh_3)_2$]$PF_6$.

**Table II.** Selected Bond Distances (Å) and Angles (deg) and Their Estimated Standard Deviations for *cct*-[$OsL_2(PPh_3)_2$]$PF_6\cdot H_2O$ and *ttt*-[$OsL_2(PPh_3)_2$]$PF_6$

| *cct*-[$OsL_2(PPh_3)_2$]$PF_6\cdot H_2O$ | | *ttt*-[$OsL_2(PPh_3)_2$]$PF_6$ | |
|---|---|---|---|
| | Distances | | |
| Os–P(1) | 2.417(3) | Os(1)–P(1) | 2.432(3) |
| Os–P(2) | 2.421(3) | Os(1)–N(1) | 2.115(9) |
| Os–N(1) | 2.103(10) | Os(1)–S(1) | 2.375(3) |
| Os–N(2) | 2.096(10) | Os(2)–P(2) | 2.424(3) |
| Os–S(1) | 2.396(3) | Os(2)–N(2) | 2.083(8) |
| Os–S(2) | 2.393(3) | Os(2)–S(2) | 2.373(3) |
| | Angles | | |
| N(1)–Os–S(1) | 67.8(3) | N(1)–Os(1)–S(1) | 68.1(2) |
| N(1)–Os–P(1) | 88.8(3) | N(1)–Os(1)–P(1) | 91.0(2) |
| S(1)–Os–P(1) | 91.7(1) | S(1)–Os(1)–P(1) | 90.4(1) |
| N(2)–Os–S(2) | 67.4(3) | N(2)–Os(2)–P(2) | 89.3(3) |
| N(2)–Os–P(1) | 90.7(3) | N(2)–Os(2)–S(2) | 68.3(2) |
| S(2)–Os–P(1) | 86.3(1) | S(2)–Os(2)–P(2) | 91.3(1) |
| N(1)–Os–P(2) | 92.5(3) | | |
| N(2)–Os–P(2) | 90.6(3) | | |
| S(1)–Os–P(2) | 87.0(1) | | |
| S(2)–Os–P(2) | 92.5(1) | | |
| P(1)–Os–P(2) | 177.6(1) | | |
| N(1)–Os–N(2) | 110.5(4) | | |
| S(1)–Os–S(2) | 114.5(1) | | |
| N(1)–Os–S(2) | 174.6(3) | | |
| N(2)–Os–S(1) | 177.0(3) | | |

**Table III.** Bulk Magnetic Moments,[a] EPR *g* Values,[b,c] Distortion Parameters, and Near-IR Transitions

| compd | $\mu_{eff}$, $\mu_B$ | $g_x$ | $g_y$ | $g_z$ | $\Delta/\lambda$ | $V/\lambda$ | $\nu_1/\lambda$ | $\nu_2/\lambda$ | $(\nu_1/\lambda)_{obsd}$[d] |
|---|---|---|---|---|---|---|---|---|---|
| *cct*-$[OsL_2(PPh_3)_2]PF_6 \cdot H_2O$ | 1.83 | 2.883 | 2.471 | 1.557 | 3.013 | −1.387 | 2.518 | 4.090 | 2.469 |
| *ttt*-$[OsL_2(PPh_3)_2]PF_6$ | 1.92 | 2.761 | 2.471 | 1.550 | 2.874 | −0.977 | 2.552 | 3.794 | 2.777 |

[a] In solid state at 298 K. [b] In 1:1 dichloromethane–toluene frozen glass (77 K). [c] Signs of *g* values are negative, negative, and positive for $g_x$, $g_y$, and $g_z$, respectively. [d] Observed frequency converted to $\nu_1/\lambda$ by setting $\lambda$ = 3000 cm$^{-1}$.

is 12.7°. The average Os–S distances in the *cct* and *ttt* isomers are respectively 2.395(3) and 2.374(3) Å. A reason for $OsL_2$ nonplanarity and significantly longer Os–S distance in the *cct* isomer can be the cis-repulsion of the two thiolato sulfur atoms. The mean Os–P distances (*cct*, 2.419 (3) Å; *ttt*, 2.428(3) Å) compare favorably with those in *trans*-$[Os(MeOCS_2)_2(PPh_3)_2]PF_6 \cdot 2H_2O$,[1] 2.439(3) Å, and *trans*-$[Os(EtSCS_2)_2(PPh_3)_2]PF_6$,[2] 2.425(1) Å.

Apart from *cct* and *ttt*, three other geometrical isomers are possible for the $OsN_2S_2P_2$ coordination sphere: *ctc*, *tcc*, and *ccc* (**3**–**5**). These have not been observed for $OsL_2(PPh_3)_2^+$. The strong steric disadvantage of the *cis*-$(PPh_3)_2$ configuration in osmium(III) complexes is well-documented.[1-3] However, the *ctc* isomer is present in the solid state of $Os^{II}L_2(PPh_3)_2$; vide infra.

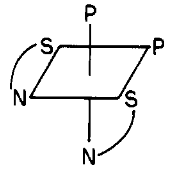

*ctc*
**3**

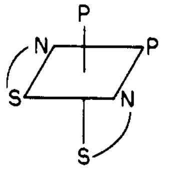

*tcc*
**4**

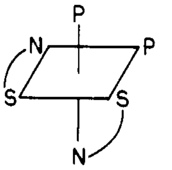

*ccc*
**5**

**C. Distortion Parameters: EPR and Near-IR Spectra.** The symmetries of red and green cations are respectively $C_i$ and $C_1$. Rhombic EPR spectra are therefore expected for both species. Such is indeed the case (Figure 1b, Table III) and the spectra (dichloromethane–toluene glass, 77 K) have been analyzed using g-tensor theory of low-spin d$^5$ ions $(t_2{}^5)$[13,14] affording measures of axial distortion ($\Delta$) which splits $t_2$ shell into e + b levels and rhombic distortion ($V$) which splits e into two nondegenerate components. The magnitudes of the $g_x$ component and the computed $\Delta$ and $V$ values for the *cct* isomer are significantly higher than those for the *ttt* isomer (Table III). Taking the spin–orbit coupling constant $\lambda$ of osmium(III)[15] to be ~3000 cm$^{-1}$, the lower energy optical transition among Kramers doublets is computed to be ~7500 in the *cct* and ~7700 cm$^{-1}$ in the *ttt* isomer. Weak transitions are indeed observed at 7400 cm$^{-1}$ in *cct* and at 8300 cm$^{-1}$ in *ttt* isomer (Figure 1 and Table I).

**D. Reduction Potentials.** In solution each isomer displays a quasireversible one-electron cyclic voltammetric response due to the osmium(III)–osmium(II) couple (Figure 4). The *cct* isomer is easier to reduce: $E_{1/2}(cct) = E_{1/2}(ttt) + 0.25$ V (Table I). Stronger back-bonding within the $OsL_2$ fragment in *cct*-$OsL_2(PPh_3)_2$ than that in the *ttt* isomer may be one of the contributing factors. For low-spin $d^5 + e \rightleftharpoons d^6$ couples $E_{1/2}$ can be correlated with back-bonding in the reduced (d$^6$) complex.[1-3,16] The superior thermodynamic stability of the *cct* isomer compared to the *ttt* isomer for osmium(II) is also reflected in the solution composition of $OsL_2(PPh_3)_2$; vide infra.

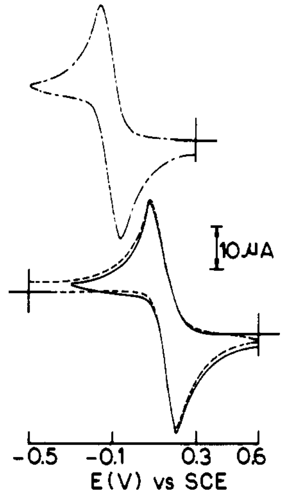

**Figure 4.** Cyclic voltammograms (scan rate 50 mV s$^{-1}$) of 10$^{-3}$ M solutions of *ctc*-$OsL_2(PPh_3)_2$ (- - -), *cct*-$[OsL_2(PPh_3)_2]PF_6 \cdot H_2O$ (—), and *ttt*-$[OsL_2(PPh_3)_2]PF_6$ (– · –) in dichloromethane (0.1 M TEAP) at a platinum electrode.

**E. Isomeric Abundance.** How do the two isomers of $OsL_2(PPh_3)_2^+$ arise during synthesis and why is their relative abundance so unequal? The possibility that one isomer arises from the other by isomerization can be ruled out. The two isomers are inert to interconversion even upon prolonged boiling in dichloromethane, chloroform and acetonitrile. This has been checked with the help of spectra, voltammetry and by isolation. The origin of the osmium(III) isomers and their population may thus be latent in the osmium(II) precursor, $OsL_2(PPh_3)_2$ itself.

In the solid state $OsL_2(PPh_3)_2$ occurs in only one form which was assigned[10] *ctc* geometry (**3**) in analogy with structurally characterized $RuL_2(PPh_3)_2$.[8] We find this analogy entirely valid since the unit cell of the latter complex is isometric with that of $OsL_2(PPh_2)_2$: orthorhombic; $a$ = 27.99(4), $b$ = 11.47(1), and $c$ = 12.31(1) Å (only crystals of moderate quality could be grown). The stability of the sterically unfavorable *cis*-$(PPh_3)_2$ configuration in the bivalent complex can be attributed to back-bonding.[1-3] However the steric and electronic factors are very delicately balanced in the present case and there is unequivocal NMR evidence that $OsL_2(PPh_3)_2$ goes over to the *trans*-$(PPh_3)_2$ situation upon dissolution.[10,11] The solution geometry is thus *cct* and/or *ttt*.

The cyclic voltammograms of the green *cct*-$OsL_2(PPh_3)_2^+$ isomer is virtually superposable on that of $OsL_2(PPh_3)_2$ (Figure 4) implying *cct* geometry for the latter. If only ~1% *ttt* isomer is present in equilibrium, it will not be observable in our voltammetric experiments but the formation of the very minor red isomer along with the predominant green isomer upon rapid metal oxidation (eq 1) will fall in place. In this plausible rationale, the oxidation process preserves the original isomer population in the form of stereorigid osmium(III). The trivalent *ttt* isomer can then be expected to isomerize upon metal reduction affording the bivalent complex $OsL_2(PPh_3)_2$ in the form that is indistinguishable with the product described above. This indeed happens rapidly and quantitatively upon reacting *ttt*-$OsL_2(PPh_3)_2^+$ with hydrazine hydrate in acetonitrile.

**F. Concluding Remarks.** The main results of this research will now be summarized. The first osmium(III) complex of pyridine-2-thiol, $OsL_2(PPh_3)_2^+$, has been isolated and structurally

---

(13) (a) Lahiri, G. K.; Bhattacharya, S.; Ghosh, B. K.; Chakravorty, A. *Inorg. Chem.* **1987**, *26*, 4324–4331. (b) Lahiri, G. K.; Bhattacharya, S.; Mukherjee, M.; Mukherjee, A. K.; Chakravorty, A. *Inorg. Chem.* **1987**, *26*, 3359–3365.

(14) (a) Bleaney, B.; O'Brien, M. C. M. *Proc. Phys. Soc. London, Sect. B* **1956**, *69*, 1216–1230. (b) Griffith, J. S. *The Theory of Transition Metal Ions*; Cambridge University Press: London, 1961; p 364.

(15) (a) Sakaki, S.; Hagiwara, N.; Yanase, Y.; Ohyoshi, A. *J. Phys. Chem.* **1978**, *82*, 1917–1920. (b) Hudson, A.; Kennedy, M. J. *J. Chem. Soc. A* **1969**, 1116–1120.

(16) Bursten, B. E. *J. Am. Chem. Soc.* **1982**, *104*, 1299–1304.

**Table IV.** Crystallographic Data for *cct*-$[OsL_2(PPh_3)_2]PF_6 \cdot H_2O$ and *ttt*-$[OsL_2(PPh_3)_2]PF_6$

| | *cct*-$[OsL_2(PPh_3)_2]PF_6 \cdot H_2O$ | *ttt*-$[OsL_2(PPh_3)_2]PF_6$ |
|---|---|---|
| chem formula | $C_{46}H_{40}N_2OF_6P_3S_2Os$ | $C_{46}H_{38}N_2F_6P_3S_2Os$ |
| fw | 1098.0 | 1080.0 |
| space group | $P2_1/c$ | $C2/c$ |
| $a$, Å | 10.265(2) | 23.615(10) |
| $b$, Å | 22.289(8) | 20.605(6) |
| $c$, Å | 19.881(10) | 19.440(5) |
| $\beta$, deg | 102.85(3) | 94.19(3) |
| $V$, Å$^3$ | 4435(3) | 9434(5) |
| $Z$ | 4 | 8 |
| $T$, °C | 22 | 22 |
| $\lambda$, Å | 0.710 73 | 0.710 73 |
| $\rho_{calcd}$, g cm$^{-3}$ | 1.645 | 1.521 |
| $\mu$, cm$^{-1}$ | 31.37 | 29.51 |
| transm coeff | 0.2143–0.2487 | 0.2321–0.2749 |
| $R^a$ | 0.0498 | 0.0446 |
| $R_w{}^b$ | 0.0546 | 0.0512 |

[a] $R = \sum||F_o| - |F_c||/\sum|F_o|$. [b] $R_w = [\sum w(|F_o| - |F_c|)^2/\sum w|F_o|^2]^{1/2}$; $w^{-1} = \sigma^2(|F_o|) + g|F_o|^2$; $g = 0.0001$ for *cct* and 0.0005 for *ttt*.

**Table V.** Atomic Coordinates (×10$^4$) and Equivalent Isotropic Displacement Coefficients (Å$^2$ × 10$^3$) for *cct*-$[OsL_2(PPh_3)_2]PF_6 \cdot H_2O$ (Estimated Standard Deviations in Parentheses)

| atom | $x$ | $y$ | $z$ | $U$(eq)$^a$ |
|---|---|---|---|---|
| Os | 2186(1) | 2288(1) | 2989(1) | 28(1) |
| S(1) | 4397(3) | 2589(1) | 2927(2) | 38(1) |
| S(2) | 1772(3) | 2298(2) | 4126(2) | 40(1) |
| P(1) | 2896(3) | 1259(1) | 3227(2) | 33(1) |
| P(2) | 1545(3) | 3330(1) | 2791(2) | 32(1) |
| P(3) | 7731(5) | 1722(2) | 380(2) | 73(2) |
| N(1) | 2530(9) | 2191(4) | 1990(5) | 33(4) |
| N(2) | 214(10) | 2056(4) | 3001(5) | 38(4) |
| C(1) | 3784(12) | 2393(5) | 2078(7) | 39(5) |
| C(2) | 4432(14) | 2390(6) | 1524(7) | 51(6) |
| C(3) | 3745(16) | 2156(6) | 909(8) | 64(7) |
| C(4) | 2455(15) | 1932(6) | 827(7) | 56(6) |
| C(5) | 1877(13) | 1953(5) | 1382(6) | 38(5) |
| C(6) | 194(11) | 2101(5) | 3660(7) | 37(5) |
| C(7) | –958(13) | 1974(6) | 3895(7) | 51(6) |
| C(8) | –2112(14) | 1871(6) | 3428(8) | 62(7) |
| C(9) | –2116(12) | 1892(6) | 2729(7) | 47(6) |
| C(10) | –948(13) | 1985(6) | 2506(7) | 43(5) |
| C(11) | –246(12) | 3474(5) | 2669(6) | 34(5) |
| C(12) | –1081(13) | 3618(6) | 2038(7) | 64(7) |
| C(13) | –2450(14) | 3675(7) | 1998(8) | 75(7) |
| C(14) | –2971(14) | 3607(6) | 2562(8) | 65(7) |
| C(15) | –2159(13) | 3478(6) | 3189(7) | 52(6) |
| C(16) | –809(12) | 3408(5) | 3235(6) | 44(5) |
| C(17) | 2223(12) | 3858(5) | 3500(6) | 35(5) |
| C(18) | 1629(14) | 4411(6) | 3500(7) | 52(6) |
| C(19) | 2157(16) | 4821(6) | 4013(8) | 70(7) |
| C(20) | 3214(17) | 4663(7) | 4541(8) | 72(7) |
| C(21) | 3796(14) | 4109(6) | 4546(7) | 58(6) |
| C(22) | 3323(12) | 3694(6) | 4019(6) | 41(5) |
| C(23) | 2118(12) | 3634(5) | 2057(6) | 33(5) |
| C(24) | 3207(12) | 4035(6) | 2145(7) | 47(6) |
| C(25) | 3766(14) | 4190(6) | 1600(8) | 61(7) |
| C(26) | 3235(17) | 3966(7) | 957(8) | 70(8) |
| C(27) | 2130(16) | 3589(6) | 842(7) | 63(7) |
| C(28) | 1595(13) | 3416(5) | 1385(6) | 45(5) |
| C(29) | 3474(13) | 847(5) | 2557(6) | 35(5) |
| C(30) | 4673(13) | 1002(6) | 2408(7) | 51(6) |
| C(31) | 5181(16) | 702(7) | 1920(8) | 73(8) |
| C(32) | 4480(20) | 231(8) | 1552(8) | 83(9) |
| C(33) | 3330(19) | 59(8) | 1713(9) | 95(10) |
| C(34) | 2816(16) | 368(7) | 2198(8) | 75(8) |
| C(35) | 1579(13) | 795(5) | 3450(6) | 37(5) |
| C(36) | 1709(14) | 547(6) | 4085(7) | 53(6) |
| C(37) | 689(17) | 204(7) | 4250(9) | 78(8) |
| C(38) | –479(16) | 117(7) | 3763(9) | 73(8) |
| C(39) | –624(14) | 359(6) | 3118(8) | 63(7) |
| C(40) | 369(14) | 700(5) | 2945(7) | 48(6) |
| C(41) | 4335(12) | 1169(6) | 3954(6) | 38(5) |
| C(42) | 4883(13) | 1632(5) | 4380(6) | 39(5) |
| C(43) | 6001(13) | 1550(6) | 4919(7) | 51(6) |
| C(44) | 6586(15) | 990(7) | 5020(7) | 63(7) |
| C(45) | 6065(15) | 533(7) | 4593(8) | 72(7) |
| C(46) | 4949(14) | 611(6) | 4072(7) | 56(6) |
| F(1) | 8766(9) | 1388(4) | 972(4) | 102(4) |
| F(2) | 7346(11) | 1138(4) | –14(5) | 139(6) |
| F(3) | 8189(18) | 2314(5) | 762(6) | 218(9) |
| F(4) | 6715(14) | 2052(5) | –193(5) | 185(7) |
| F(5) | 8837(13) | 1809(7) | –29(6) | 191(8) |
| F(6) | 6691(12) | 1623(9) | 787(7) | 245(11) |
| O(1W) | 718(16) | 384(7) | 525(9) | 260(14) |

[a] Equivalent isotropic $U$ defined as one-third of the trace of the orthogonalized $\mathbf{U}_{ij}$ tensor.

characterized (as $PF_6^-$ salts) in two geometrically isomeric forms in which the grossly planar $OsL_2$ fragment has cis (green form) and trans (red form) configurations; the $PPh_3$ ligands lie trans to each other in both forms. No isomers with the sterically hindered *cis*-$(PPh_3)_2$ configurations are observed. Formation of the green and red isomers in very unequal proportions (only ~1% red form) is believed to arise from the geometrical nature of the synthetic precursor $OsL_2(PPh_3)_2$ in solution.

The osmium(III)–osmium(II) reduction potentials differ significantly for the two isomers (green > red). Analyses of EPR spectra reveal sizable splitting of the $t_2$ shell in both isomers and this is realized in practice in the form of a ligand field transition in near-IR region. Calculated and observed band positions agree well.

## Experimental Section

**Materials.** Osmium tetroxide obtained from Arora-Matthey, Calcutta, India, was reacted with HBr to afford $(NH_4)_2OsBr_6$[17] which was converted to $Os(PPh_3)_3Br_2$ as reported.[18] Pyridine-2-thiol was purchased from Aldrich. The preparation of tetraethylammonium perchlorate and the purification of solvents for electrochemical and spectroscopic work were as done before.[1] All other chemicals and solvents were of reagent grade and used without further purification.

**Physical Measurements.** Spectroscopic data were obtained with the following spectrometers: vis–near-IR, Hitachi 330; IR, Perkin-Elmer 783; X-band EPR, Varian E-109C. Magnetic susceptibilities were measured on a PAR-155 vibrating-sample magnetometer fitted with a Walker Scientific magnet. Solution electrical conductivity was measured by using a Philips PR 9500 bridge. Electrochemical and microanalytical measurements were done as before.[1]

**Preparation of Complexes. Bis(pyridine-2-thiolato)bis(triphenylphosphine)osmium(II), $OsL_2(PPh_3)_2$.** To a warm solution of $Os(PPh_3)_3Br_2$ (300 mg, 0.27 mmol) in ethanol (40 mL) was added pyridine-2-thiol (75 mg, 0.68 mmol). The mixture was refluxed for 1 h. Upon cooling, an orange microcrystalline solid separated which was collected by filtration, washed thoroughly with ethanol, and dried in vacuo over $P_4O_{10}$. The yield was 98%. The previously reported method was based on $Os(PPh_3)_3H_4$.[10]

Anal. Calcd for *ctc*-$OsL_2(PPh_3)_2$, $OsC_{46}H_{38}N_2S_2P_2$: C, 59.09; H, 4.07; N, 3.00. Found: C, 59.17; H, 4.05; N, 3.08.

**Hydrated Bis(pyridine-2-thiolato)bis(triphenylphosphine)osmium(III) Hexafluorophosphate, $[OsL_2(PPh_3)_2]PF_6 \cdot nH_2O$. (a) Isomeric Mixture.** To a solution of 200 mg (0.22 mmol) of $OsL_2(PPh_3)_2$ in 30 mL of dichloromethane–acetonitrile (1:10) was added 190 mg (0.30 mmol) of ceric ammonium sulfate dissolved in 20 mL of water. The mixture was stirred at room temperature for 20 min. The color of the solution became green. The reaction mixture was then filtered and the filtrate reduced to 10 mL under reduced pressure. A saturated aqueous solution of $NH_4PF_6$ (10 mL) was added. The green solid thus obtained was collected by filtration, washed with water and dried in vacuo over $P_4O_{10}$. The crude product was dissolved in a minimum volume of dichloromethane and was subjected to chromatography on a silica gel (60–120 mesh, BDH) column (20 × 1) cm. On elution with benzene-acetonitrile (9:1) the mixture of isomers moved out very fast and was collected. The crystalline residue (yield 95%) obtained by evaporation of solvent was used for the next operation.

**(b) Separation of Two Isomers.** Hexane (30 mL) was layered over a solution of 148 mg of the above residue taken in 15 mL of pure

---

(17) Dwyer, F. P.; Hogarth, J. W. *Inorg. Synth.* **1957**, *5*, 204–209.

(18) Hoffman, P. R.; Caulton, K. G. *J. Am. Chem. Soc.* **1975**, *97*, 4221–4228.

**Table VI.** Atomic Coordinates ($\times 10^4$) and Equivalent Isotropic Displacement Coefficients ($Å^2 \times 10^3$) for *ttt*-$[OsL_2(PPh_3)_2]PF_6$ (Estimated Standard Deviations in Parentheses)

| atom | *x* | *y* | *z* | *U*(eq)[a] |
|---|---|---|---|---|
| Os(1) | 2500 | 2500 | 5000 | 27(1) |
| P(1) | 1487(1) | 2362(1) | 5101(1) | 34(1) |
| S(1) | 2687(1) | 2186(2) | 6170(1) | 42(1) |
| N(1) | 2633(3) | 1489(4) | 5100(4) | 33(3) |
| C(1) | 2715(5) | 1422(5) | 5805(5) | 38(3) |
| C(2) | 2796(6) | 832(7) | 6109(7) | 56(4) |
| C(3) | 2816(7) | 286(9) | 5677(9) | 73(6) |
| C(4) | 2728(8) | 372(6) | 4959(8) | 67(5) |
| C(5) | 2613(6) | 975(6) | 4684(6) | 45(4) |
| C(6) | 1326(5) | 1519(6) | 5002(6) | 46(4) |
| C(7) | 1307(6) | 1121(7) | 5591(9) | 67(5) |
| C(8) | 1269(8) | 439(9) | 5510(12) | 83(8) |
| C(9) | 1214(8) | 187(10) | 4831(14) | 95(8) |
| C(10) | 1218(8) | 558(11) | 4285(11) | 85(8) |
| C(11) | 1294(6) | 1200(7) | 4358(8) | 60(5) |
| C(12) | 998(5) | 2838(7) | 4502(5) | 44(4) |
| C(13) | 597(6) | 2549(9) | 4021(7) | 72(5) |
| C(14) | 248(8) | 2950(13) | 3621(8) | 94(8) |
| C(15) | 251(8) | 3587(14) | 3688(10) | 105(9) |
| C(16) | 638(8) | 3863(10) | 4144(12) | 90(8) |
| C(17) | 993(6) | 3501(8) | 4569(8) | 64(5) |
| C(18) | 1207(4) | 2614(6) | 5911(5) | 39(3) |
| C(19) | 660(6) | 2395(7) | 6064(6) | 57(5) |
| C(20) | 417(6) | 2608(9) | 6645(7) | 71(6) |
| C(21) | 718(6) | 3021(9) | 7108(7) | 66(5) |
| C(22) | 1236(6) | 3239(8) | 6946(6) | 62(5) |
| C(23) | 1497(6) | 3042(6) | 6361(5) | 46(4) |
| Os(2) | 2500 | 2500 | 0 | 34(1) |
| P(2) | 1508(1) | 2738(2) | 127(1) | 44(1) |
| P(3) | 2797(2) | 5778(2) | 2587(2) | 68(1) |
| S(2) | 2325(1) | 1368(2) | 49(2) | 46(1) |
| N(2) | 2277(4) | 2117(4) | −974(4) | 38(3) |
| C(24) | 2186(5) | 1474(6) | −833(6) | 47(4) |
| C(25) | 2040(7) | 1017(8) | −1352(7) | 61(5) |
| C(26) | 1955(7) | 1250(8) | −2033(7) | 64(5) |
| C(27) | 2030(7) | 1903(8) | −2156(6) | 62(5) |
| C(28) | 2196(6) | 2323(7) | −1630(5) | 48(4) |
| C(29) | 1418(6) | 3032(11) | 984(7) | 76(7) |
| C(30) | 1332(9) | 3684(14) | 1082(8) | 107(10) |
| C(31) | 1295(10) | 3880(18) | 1787(15) | 161(15) |
| C(32) | 1336(13) | 3491(34) | 2319(17) | 222(27) |
| C(33) | 1407(12) | 2845(31) | 2198(12) | 190(23) |
| C(34) | 1469(7) | 2595(15) | 1545(7) | 127(12) |
| C(35) | 1011(6) | 2065(7) | −30(8) | 62(5) |
| C(36) | 710(9) | 1746(10) | 457(12) | 99(8) |
| C(37) | 311(9) | 1211(12) | 222(19) | 116(12) |
| C(38) | 247(11) | 1041(14) | −417(28) | 153(18) |
| C(39) | 552(10) | 1354(13) | −867(16) | 123(11) |
| C(40) | 918(7) | 1843(8) | −690(10) | 79(7) |
| C(41) | 1138(5) | 3344(6) | −443(6) | 43(4) |
| C(42) | 574(7) | 3467(8) | −360(7) | 65(5) |
| C(43) | 267(9) | 3908(10) | −767(10) | 83(7) |
| C(44) | 549(9) | 4227(8) | −1293(8) | 76(7) |
| C(45) | 1094(8) | 4105(8) | −1390(7) | 66(6) |
| C(46) | 1407(6) | 3650(7) | −961(6) | 50(4) |
| F(1) | 2973(10) | 5145(8) | 2962(8) | 175(9) |
| F(2) | 2618(8) | 6407(8) | 2190(7) | 154(8) |
| F(3) | 2235(11) | 5469(14) | 2400(22) | 318(22) |
| F(4) | 3341(10) | 6095(10) | 2755(20) | 296(19) |
| F(5) | 2558(13) | 6081(11) | 3217(11) | 259(16) |
| F(6) | 2943(14) | 5472(9) | 1941(7) | 246(15) |

[a] Equivalent isotropic *U* defined as one-third of the trace of the orthogonalized $\mathbf{U}_{ij}$ tensor.

dichloromethane. Two types of crystals (green and red) deposited within a few days upon diffusion and slow evaporation. The remaining solvent was colorless and was removed by decantation. The two types of crystals were separated by hand-picking using a microscope whenever necessary affording 1.55 mg of the pure red form and 146.32 mg of the pure green form. The procedure was repeated several times with new batches of isomeric mixtures to collect a sizeable amount of the red isomer required for various studies.

Anal. Calcd for green isomer, *cct*-$[OsL_2(PPh_3)_2]PF_6 \cdot H_2O$, $OsC_{46}H_{40}N_2S_2P_3F_6O$: C, 50.27; H, 3.64; N, 2.55. Found: C, 50.42; H, 3.67; N, 2.53. Calcd for red isomer, *ttt*-$[OsL_2(PPh_3)_2]PF_6$, $OsC_{46}H_{38}N_2S_2P_3F_6$: C, 51.11; H, 3.52; N, 2.59. Found: C, 51.10; H, 3.55; N, 2.57. In acetonitrile solution molar conductivities ($\Lambda$) of green and red isomers are 142 and 128 $\Omega^{-1}$ cm$^2$ M$^{-1}$, respectively.

**Reduction of $[OsL_2(PPh_3)_2]PF_6 \cdot nH_2O$ by Hydrazine Hydrate.** A 20 mg portion of *ttt*-$[OsL_2(PPh_3)_2]PF_6$ was dissolved in acetonitrile (5 mL). A solution of hydrazine hydrate (0.1 mL) in acetonitrile (5 mL) was then added under stirring. The color of the solution immediately changed from red to orange-yellow. Upon removal of solvent an orange crystalline solid was isolated which was washed with water and dried in vacuo over $P_4O_{10}$. This product was found to be identical with $OsL_2(PPh_3)_2$ reported above in all respects: elemental analyses, unit cell dimensions, electronic spectra and electrochemistry. The yield was essentially quantitative. The same product was also obtained when *ttt*-$[OsL_2(PPh_3)_2]PF_6$ was replaced by *cct*-$[OsL_2(PPh_3)_2]PF_6 \cdot H_2O$ in the above experiment (here color changes from green to orange-yellow upon addition of the reductant).

**X-ray Structure Determination.** Data collection was performed on a Nicolet R3m/V automated diffractometer using graphite-monochromated Mo K$\alpha$ radiation ($\lambda$ = 0.710 73 Å). Significant crystal data and data collection parameters are listed in Table IV. The unit cell parameters were determined by a least-squares fit of 25 reflections selected from rotation photographs and data collection was made over the $2\theta$ range 2–52° using the $\omega$-scan method. In both the cases, two check reflections were measured after every 98 reflections during data collection to monitor crystal stability. No significant intensity reduction was found in the 95 and 80 h of exposure to X-rays for the *cct* and *ttt* isomers, respectively. All data were corrected for Lorentz–polarization effects, and an empirical absorption correction was done on the basis of azimuthal scans.[19] For the *cct* isomer, 11 320 data were collected, of which 8660 were unique and 4371 satisfying the $I > 3\sigma(I)$ criterion were used for structure solution. For the *ttt* isomer the corresponding numbers are 9693, 9203 and 3822, respectively. The space group of the *cct* isomer was uniquely settled by systematic absences. For the *ttt* isomer space group is either *Cc* or *C*2/*c*. Successful structure solution was achieved with the latter space group (*C*2/*c*).

All calculations for data reduction, structure solution, and refinement were done on a MicroVAX II computer using the SHELXTL-PLUS[20] program package. The metal positions were located from Patterson maps and the rest of the non-hydrogen atoms emerged from difference Fourier syntheses. The structures were then refined by full-matrix least-squares procedures. All non-hydrogen atoms were refined anisotropically and hydrogen atoms were added at their respective calculated positions with fixed $U$ = 0.08 Å$^2$ in the final cycle of refinement. The final convergent refinement gave residuals as stated in Table IV. The highest difference Fourier peaks were 0.78 and 0.87 e Å$^{-3}$, respectively, for the *cct* and *ttt* isomers near the metal atoms. Atomic coordinates and isotropic thermal parameters for the two structures are collected in Tables V and VI.

**Unit Cell Dimensions of $OsL_2(PPh_3)_2$.** Single crystals were grown by slow diffusion of dichloromethane solution into hexane followed by slow evaporation. Unit cell parameters were determined with a crystal of dimensions 0.10 × 0.12 × 0.06 mm$^3$ by the least-squares fit of 20 machine-centered reflections having $2\theta$ values in the range 12–25°. Dimensions of the orthorhombic cell have already been stated in the text.

**Acknowledgment.** Crystallography was done at the National Single Crystal Diffractometer Facility, Department of Inorganic Chemistry, Indian Association for the Cultivation of Science. Financial support received from the Department of Science and Technology, New Delhi, India, and the Council of Scientific and Industrial Research, New Delhi, India, is acknowledged.

**Supplementary Material Available:** Full listings of bond distances (Tables VII and VIII), bond angles (Tables IX and X), anisotropic thermal parameters (Tables XI and XII), and hydrogen atom coordinates (Tables XIII and XIV) and a view of the *cct* lattice down the *b* axis (Figure 5) (21 pages). Ordering information is given on any current masthead page.

---

(19) North, A. C. T.; Philips, D. C.; Mathews, F. S. *Acta Crystallogr., Sect. A* **1968**, *A24*, 351–359.

(20) Sheldrick, G. M. *SHELXTL-Plus 88, Structure Determination Software Programs*; Nicolet Instrument Corp.: 5225-2 Verona Rd., Madison, WI 53711, 1988.